ÉCOLE POLYTECHNIQUE FÉDÉRALE DE LAUSANNE

MATHICSE

Mathematics Institute of Computational Science and Engineering

School of Basic Sciences - Section of Mathematics

MATHICSE Technical Report

Nr. 37.2014

September 2014

Parallel algorithms for tensor completion in the CP format

Lars Karlsson, Daniel Kresser, André Uschmajew

http://mathicse.epfl.ch

Phone: +41 21 69 37648

Address:
EPFL - SB - MATHICSE (Bâtiment MA)
Station 8 - CH-1015 - Lausanne - Switzerland

Fax: +41 21 69 32545

Parallel Algorithms for Tensor Completion in the CP Format

Lars Karlsson

Department of Computing Science, Umeå University, 901 87 Umeå, Sweden

Daniel Kressner

MATHICSE-ANCHP SMA, EPF Lausanne, 1015 Lausanne, Switzerland

André Uschmajew

Institute for Numerical Simulation, Wegelerstraße 6, 53115 Bonn, Germany

Abstract

Low-rank tensor completion addresses the task of filling in missing entries in multi-dimensional data. It has proven its versatility in numerous applications, including context-aware recommender systems and multivariate function learning. To handle large-scale datasets and applications that feature high dimensions, the development of distributed algorithms is central. In this work, we propose novel, highly scalable algorithms based on a combination of the canonical polyadic (CP) tensor format with block coordinate descent methods. Although similar algorithms have been proposed for the matrix case, the case of higher dimensions gives rise to a number of new challenges and requires a different paradigm for data distribution. The convergence of our algorithms is analyzed and numerical experiments illustrate their performance on distributed-memory architectures for tensors from a range of different applications.

Keywords: low-rank tensor completion, canonical tensor format, cyclic coordinate descent, alternating least squares, parallel tensor completion, parallel cyclic coordinate descent, parallel alternating least squares

1. Introduction

Tensor completion is the task of completing multi-dimensional data with missing values. To make this task well-posed, rank constraints are typically imposed on the tensor. Unlike in the matrix case, the definition of the rank of a tensor is not unique. In this work, we focus on the CP format, in which the tensor is represented as a sum of rank-one tensors.

Email addresses: larsk@cs.umu.se (Lars Karlsson), daniel.kressner@epfl.ch (Daniel Kressner), uschmajew@ins.uni-bonn.de (André Uschmajew)

More specifically, following the notation in [1], the CP format of a tensor $\mathcal{X} \in \mathbb{R}^{I_1 \times I_2 \times \cdots \times I_N}$ of order N takes the form

$$\mathcal{X} = \sum_{\ell=1}^{L} \mathbf{x}_\ell^{(1)} \circ \mathbf{x}_\ell^{(2)} \circ \cdots \circ \mathbf{x}_\ell^{(N)}, \qquad \mathbf{x}_\ell^{(n)} \in \mathbb{R}^{I_n}, \tag{1}$$

where $\circ$ denotes the vector outer product. The smallest L, for which (1) is possible, is called the tensor rank of $\mathcal{X}$.

Let $\mathcal{A}$ be a data tensor with known entries in an index set Ω, that is, the entry $a_{i_1 \cdots i_N}$ of $\mathcal{A}$ is known if and only if $\mathbf{i} = (i_1, \ldots, i_N) \in \Omega$. Then we seek to fit the components $\mathbf{x}_\ell^{(n)}$ of (1) for a tensor $\mathcal{X}$ of tensor rank L to this given data. Letting P_Ω denote the orthogonal projection onto Ω, this can be addressed by solving the optimization problem

$$\min \left\| P_\Omega\Big(\mathcal{A} - \sum_{\ell=1}^{L} \mathbf{x}_\ell^{(1)} \circ \mathbf{x}_\ell^{(2)} \circ \cdots \circ \mathbf{x}_\ell^{(N)}\Big) \right\|_2^2 + \lambda \sum_{\ell=1}^{L} \sum_{n=1}^{N} \left\| \mathbf{x}_\ell^{(n)} \right\|_2^2, \tag{2}$$

where $\lambda \geq 0$ is a regularization parameter. The aim of this work is to propose and analyze parallel methods for solving (2). Applications that require the completion of tensors (that, is $N > 2$) include context-aware recommender systems [2], multivariate function learning [3], reconstruction of hyperspectral images [4], and seismic inversion [5].

For $N = 2$ the problem (2) is an instance of the well-known matrix completion problem. Among the many algorithms proposed in the literature, parallel approaches have been proposed based on ALS (alternating least-squares) [6, 7], CCD (cyclic coordinate descent) [8, 9, 10] and SGD (stochastic gradient descent) [6, 11, 12].

For $N > 2$, the problem of tensor factorization into CP format is a well-studied subject for complete data, see [1] and references therein. In contrast, the case of incomplete data (that is, tensor completion in the CP format) has received much less attention. Most existing algorithms [2, 13, 14] use a combination of standard techniques (ALS, nonlinear CG, ...) with weight matrices or imputation in order to deal with the missing data. In [15], an alternating proximal gradient method was applied to (2), but with nonnegativity constraints. To the best of our knowledge, no parallel algorithm has been proposed for (2). For the case of complete data, Phan and Cichoki [16] have studied the parallelization of ALS based on local CP models.

Block coordinate descent (BCD) techniques like ALS are efficient for tensor optimization problems because they exploit the multi-linearity of the outer product. The CP format (1) is linear with respect to each of the factor matrices

$$\mathbf{X}^{(n)} = \left[\mathbf{x}_1^{(n)}, \mathbf{x}_2^{(n)}, \ldots, \mathbf{x}_L^{(n)}\right] \in \mathbb{R}^{I_n \times L}, \tag{3}$$

which collect all vectors $\mathbf{x}_\ell^{(n)}$ corresponding to a fixed mode $n = 1, \ldots, N$. Each step of ALS updates one of the factor matrices, which requires the solution of I_n normal equations of size $L \times L$. To mitigate the cost incurred by these normal equations for larger L and to improve scalability, Yu et al. [9, 10] recently proposed a simpler block coordinate method for the

matrix completion problem ($N = 2$), which they termed CCD++. In this paper, we generalize CCD++ to the tensor case. In contrast to ALS, this method considers a "feature-wise" [9, 10] partition into the block variables $\mathbf{Y}_\ell = \left[\mathbf{x}_\ell^{(1)}, \mathbf{x}_\ell^{(2)}, \ldots, \mathbf{x}_\ell^{(N)}\right]$ corresponding to the L terms in the sum (1). Each step of CCD++ updates one of these block variables, which amounts to a rank-one approximation and is addressed by performing $T \geq 1$ iterations of ALS. The entries of a single vector $\mathbf{x}_\ell^{(n)}$ can be updated in parallel by an explicit formula without matrix inversion, resulting in a cyclic coordinate descent method operating on scalar variables.

In this work, we develop and analyze novel parallel algorithms for tensor completion, based on ALS and CCD++. As explained in more detail in Section 3, the transition from the matrix case [9, 10] to the tensor cases pose a number of new challenges for load balancing and data distribution.

2. Description of algorithms

In this section, we give a detailed description of ALS and the CCD++ method for solving (2).

2.1. ALS

One step of ALS consists of optimizing a single factor matrix (3), while keeping the others fixed. To derive the corresponding equations, we first recall the CP format (1) in its entry-wise form:

$$x_{i_1 \cdots i_N} = \sum_{\ell=1}^{L} \prod_{n=1}^{N} \left[\mathbf{x}_\ell^{(n)}\right]_{i_n}.$$

Hence, the $\hat{n}$th factor matrix that minimizes (2) while keeping all other factor matrices fixed is obtained from the solution of the $I_{\hat{n}}$ optimization problems

$$\min_{z_1, z_2, \ldots, z_L} \sum_{\substack{\mathbf{i} \in \Omega \\ i_{\hat{n}} = \hat{\imath}}} \left(a_{\mathbf{i}} - \sum_{\ell=1}^{L} z_\ell \prod_{\substack{n=1 \\ n \neq \hat{n}}}^{N} \left[\mathbf{x}_\ell^{(n)}\right]_{i_n} \right)^2 + \lambda \sum_{\ell=1}^{L} z_\ell^2, \qquad \hat{\imath} = 1, \ldots, I_{\hat{n}}. \tag{4}$$

Let $|\Omega_{\hat{n},\hat{\imath}}|$ be the number of known entries satisfying $i_{\hat{n}} = \hat{\imath}$. Stacking these entries in a vector $\mathbf{a}_{\hat{n},\hat{\imath}}$, and arranging the partial products $\prod_{n \neq \hat{n}} \left[\mathbf{x}_\ell^{(n)}\right]_{i_n}$ into an $|\Omega_{\hat{n},\hat{\imath}}| \times L$ matrix $H_{\hat{n},\hat{\imath}}$ accordingly, (4) becomes

$$\min_{\mathbf{z}} \|\mathbf{a}_{\hat{n},\hat{\imath}} - H_{\hat{n},\hat{\imath}}\mathbf{z}\|_2^2 + \lambda \|\mathbf{z}\|_2^2.$$

When $\lambda > 0$, the solution to this least-squares problem is unique, and given by

$$\mathbf{z}^* = (H_{\hat{n},\hat{\imath}}^{\mathsf{T}} H_{\hat{n},\hat{\imath}} + \lambda I)^{-1} H_{\hat{n},\hat{\imath}}^{\mathsf{T}} \mathbf{a}_{\hat{n},\hat{\imath}}. \tag{5}$$

Thus, the coordinate update rule for the $\hat{\imath}$th row of the $\hat{n}$th factor matrix consists of replacing the entries $\left[\mathbf{x}_\ell^{(\hat{n})}\right]_{\hat{\imath}}$ for $\ell = 1, 2, \ldots, L$ with the entries of $\mathbf{z}^*$ given by (5). As the update does not depend on other entries than those in slice $i_{\hat{n}} = \hat{\imath}$, all slices can be updated in parallel.

The overall ALS procedure is summarized as Algorithm 1. The choice of starting vectors $\mathbf{x}_\ell^{(n)}$ is random in our experiments. By (4), they should certainly not be initialized with all zeros.

Algorithm 1: ALS

```
Initialize all vectors x_ℓ^(n);
for each iteration do
    for n̂ = 1, 2, ..., N do
        for î = 1, 2, ..., I_n̂ do in parallel
            Update L entries [x_ℓ^(n̂)]_î, ℓ = 1, 2, ..., L, using (5);
```

2.2. CCD++

One step of CCD++ consists of optimizing a single term in the sum (1), while keeping the others fixed. To update the $\hat{\ell}$th term $\mathbf{x}_{\hat{\ell}}^{(1)} \circ \mathbf{x}_{\hat{\ell}}^{(2)} \circ \cdots \circ \mathbf{x}_{\hat{\ell}}^{(N)}$, one has to find a best rank-one approximation of

$$\mathcal{A} - \sum_{\ell \neq \hat{\ell}} \mathbf{x}_{\ell}^{(1)} \circ \mathbf{x}_{\ell}^{(2)} \circ \cdots \circ \mathbf{x}_{\ell}^{(N)}.$$

This is done approximately, by performing a few iterations of rank-one ALS.

The $\hat{n}$th step of rank-one ALS consists of minimizing (2) with respect to the single vector $\mathbf{x}_{\hat{\ell}}^{(\hat{n})}$. According to (5), we replace the $\hat{\imath}$th entry of $\mathbf{x}_{\hat{\ell}}^{(\hat{n})}$ by

$$z^* = \frac{\displaystyle\sum_{\substack{\mathbf{i}\in\Omega \\ i_{\hat{n}}=\hat{\imath}}} \left(a_{\mathbf{i}} - \sum_{\substack{\ell=1 \\ \ell\neq\hat{\ell}}}^{L} \prod_{n=1}^{N} \left[\mathbf{x}_{\ell}^{(n)}\right]_{i_n} \right) \prod_{\substack{n=1 \\ n\neq\hat{n}}}^{N} \left[\mathbf{x}_{\hat{\ell}}^{(n)}\right]_{i_n}}{\lambda + \displaystyle\sum_{\substack{\mathbf{i}\in\Omega \\ i_{\hat{n}}=\hat{\imath}}} \left(\prod_{\substack{n=1 \\ n\neq\hat{n}}}^{N} \left[\mathbf{x}_{\hat{\ell}}^{(n)}\right]_{i_n} \right)^2}. \tag{6}$$

This can be done for all $\hat{\imath} = 1, 2, \ldots, I_{\hat{n}}$ in parallel.

In principle, the block coordinate update rule (6) for $\mathbf{x}_{\hat{\ell}}^{(\hat{n})}$ can be applied in any order, but the choice of this order will affect convergence. Following the matrix case [9, 10], CCD++ optimizes all entries for a given rank-one term ($\hat{\ell}$), by sweeping through $\hat{n} = 1, 2, \ldots, N$ possibly multiple times, before moving on to the next rank-one term. This leads to the nested loop structure shown in Algorithm 2.

Efficient evaluation of (6). The quantities

$$r_{\mathbf{i}} := a_{\mathbf{i}} - \sum_{\substack{\ell=1 \\ \ell\neq\hat{\ell}}}^{L} \prod_{n=1}^{N} \left[\mathbf{x}_{\ell}^{(n)}\right]_{i_n}, \qquad \mathbf{i} \in \Omega, \tag{7}$$

appearing in the numerator of (6) do not depend on $\hat{n}$. Therefore, they need to be evaluated only once when sweeping through $\hat{n} = 1, 2, \ldots, N$. This trick effectively reduces the number

Algorithm 2: CCD++

Initialize all vectors $\mathbf{x}_\ell^{(n)}$ and $\mathcal{R}$ for $\hat{\ell} = 1$ using (7);
for *each outer iteration* **do**
  for $\hat{\ell} = 1, 2, \ldots, L$ **do**
    for *each inner iteration* **do**
      for $\hat{n} = 1, 2, \ldots, N$ **do**
        for $\hat{\imath} = 1, 2, \ldots, I_{\hat{n}}$ **do in parallel**
          Update entry $\left[\mathbf{x}_{\hat{\ell}}^{(\hat{n})}\right]_{\hat{\imath}}$ using (6);
      Update $\mathcal{R}$ in parallel using (8) with $\hat{\ell}_{\text{old}} = \hat{\ell}$ and $\hat{\ell}_{\text{new}} = 1 + (\hat{\ell} \bmod L)$;

of evaluations by a factor of $1/N$, at the expense of storing all these quantities in a sparse tensor $\mathcal{R}$ with the same sparsity pattern as $\mathcal{A}$.

When moving from one rank-one term to the next, the value of $\hat{\ell}$ changes from $\hat{\ell}_{\text{old}}$ to $\hat{\ell}_{\text{new}}$. Consequently, the sum that appears in the definition (7) of $r_{\mathbf{i}}$ loses one term (corresponding to $\hat{\ell}_{\text{new}}$) and gains one term (corresponding to $\hat{\ell}_{\text{old}}$). To compensate for these changes, we perform the update

$$r_{\mathbf{i}} \leftarrow r_{\mathbf{i}} - \prod_{n=1}^{N} \left[\mathbf{x}_{\hat{\ell}_{\text{old}}}^{(n)}\right]_{i_n} + \prod_{n=1}^{N} \left[\mathbf{x}_{\hat{\ell}_{\text{new}}}^{(n)}\right]_{i_n} . \tag{8}$$

This natural rule was also used in [9, 10] for matrices ($N = 2$). Especially for large ranks L, it is much more efficient than recomputing $\mathcal{R}$ from scratch whenever $\hat{\ell}$ changes.

Inner iterations. Using more than one inner iteration in Algorithm 2 can sometimes be beneficial; it potentially allows to make progress without having to perform the update (8) of $\mathcal{R}$. For the matrix case, Yu et al. [9, 10] proposed an adaptive scheme that selects the number of inner iterations based on the observed convergence behavior, leading to a considerable improvement of the performance. However, to simplify the interpretation of the results, we use only one inner iteration in our numerical experiments. As demonstrated in the supplementary material, choosing two inner iterations in CCD++ does not necessarily lead to improved performance in the tensor case.

2.3. Convergence

In the following, we provide a convergence analysis of Algorithm 2 for the case of one inner iteration. Our analysis is based on recent results [15] concerning the convergence of cyclic BCD methods applied to multi-convex real-analytic functions.

We treat the parameters $\mathbf{x}_\ell^{(n)}$ of our model (1) as disjoint blocks of a single array $\mathbf{X}$ arranged in CCD++ order, that is,

$$\mathbf{X} = \left[\mathbf{x}_1^{(1)}, \ldots, \mathbf{x}_1^{(N)}, \mathbf{x}_2^{(1)}, \ldots, \mathbf{x}_2^{(N)}, \ldots, \mathbf{x}_L^{(1)}, \ldots, \mathbf{x}_L^{(N)}\right].$$

Moreover, we split the objective function (2) into the model error

$$E(\mathbf{X}) = \left\| P_\Omega\Big(\boldsymbol{\mathcal{A}} - \sum_{\ell=1}^{L} \mathbf{x}_\ell^{(1)} \circ \mathbf{x}_\ell^{(2)} \circ \cdots \circ \mathbf{x}_\ell^{(N)}\Big) \right\|_2^2 \tag{9}$$

and the squared norm $\|\mathbf{X}\|_2^2 = \sum_{\ell=1}^{L} \sum_{n=1}^{N} \left\|\mathbf{x}_\ell^{(n)}\right\|_2^2$ of the representation parameters. The CCD++ algorithm is simply the cyclic BCD method with exact line search applied to the objective function

$$f_\lambda(\mathbf{X}) = E(\mathbf{X}) + \lambda \|\mathbf{X}\|_2^2. \tag{10}$$

The case $\lambda = 0$ (no regularization) leads to a number of difficulties in the analysis, due to the lack of closedness [17] and the scaling indeterminacy [18] of the CP format. To avoid these difficulties, we assume that regularization is present ($\lambda > 0$). Then the sublevel sets of f_λ are bounded so that (2) has at least one globally optimal solution. Although we cannot ensure that the algorithm will find such a global solution, the multi-convexity of the objective function allows us to prove convergence to a critical point.

Proposition 1. *Assume $\lambda > 0$ and let $\mathbf{X}_k$ denote the parameter array produced by k outer iterations of Algorithm 2 (using one inner iteration). Then the sequence $(\mathbf{X}_k)$ converges to a critical point $\mathbf{X}_*$ of f_λ and $\|\mathbf{X}_k - \mathbf{X}_*\|_2 \leq Ck^{-\alpha}$ for constants $C > 0$ and $\alpha \in (1, \infty)$. If, additionally, the Hessian $\nabla^2 f_\lambda(\mathbf{X}_*)$ is positive definite, then $\mathbf{X}_*$ is a local minimum, and the convergence is asymptotically Q-linear: $\|\mathbf{X}_k - \mathbf{X}_*\|_2 \leq q\|\mathbf{X}_{k-1} - \mathbf{X}_*\|_2$ for $q \in (0, 1)$ and sufficiently large k. The same statements hold for Algorithm 1.*

Proof. As noted above, Algorithm 2 is cyclic BCD applied to the real-analytic function f_λ. Consequently, the first part follows from Theorem 2.8 in [15], provided that the optimization problem with respect to any of the block variables $\mathbf{x}_\ell^{(n)}$ is strongly convex with a lower bound on the Hessian independent of the current iterate. To see that this is indeed the case, let $\varphi(\mathbf{x}_\ell^{(n)})$ denote the restriction of f_λ to $\mathbf{x}_\ell^{(n)}$ with all other blocks fixed. As the restriction of E in (9) to $\mathbf{x}_\ell^{(n)}$ is a non-negative quadratic function, it follows directly from (10) that the smallest eigenvalue of $\nabla^2\varphi$ is bounded from below by λ at any point. The convergence rate is as stated in Theorem 2.9 in [15]. Although this theorem also covers the second part (that is, the case of a positive definite Hessian), it is worth noting that this part follows from textbook results [19, Section 10.3]. The arguments for Algorithm 1 are the same, as ALS is cyclic BCD with respect to the block variables (3). □

The positive definiteness of $\nabla^2 f_\lambda(\mathbf{X}_*)$ can be enforced by a sufficiently strong regularization.

Proposition 2. *Fix $R > 0$. There exists $\lambda_0 > 0$ such that for all $\lambda \geq \lambda_0$ and all starting points $\mathbf{X}_0$ with $\|\mathbf{X}_0\|_2 \leq R$ the following holds: The Hessian at all points in the sublevel set $\mathcal{L}_\lambda(\mathbf{X}_0) = \{\mathbf{X} \mid f_\lambda(\mathbf{X}) \leq f_\lambda(\mathbf{X}_0)\}$ has eigenvalues bounded from below by λ, which ensures linear convergence according to Theorem 1.*

Proof. Let $\mathbf{X} \in \mathcal{L}_\lambda(\mathbf{X}_0)$. By (10), the fact that E is never negative implies $\|\mathbf{X}\|_2^2 \leq E(\mathbf{X}_0)/\lambda + R \leq E^*/\lambda + R$, where E^* is the maximum of E on the zero-centered ball of radius R. Let σ_λ denote the mimimum of the smallest eigenvalues of ∇E^2 on a zero-centered ball of radius $(E^*/\lambda + R)^{1/2}$. Then the smallest eigenvalue of $\nabla^2 f_\lambda(\mathbf{X})$ is bounded from below by $\sigma_\lambda + 2\lambda$. This implies the assertion, considering that σ_λ does not decrease when λ increases. □

The convexification of the problem on a sublevel set suggested by Proposition 2 is likely to change its qualitative properties. For completeness, we note that the global convergence of cyclic BCD for strongly convex problems at an asymptotically linear rate has been obtained in earlier works like [20].

3. Parallel algorithms

In this section, we present parallel formulations of ALS (Algorithm 1) and CCD++ (Algorithm 2) in the message-passing paradigm.

The parallel tensor completion algorithms proposed below fundamentally differ from previously published algorithms for the matrix case. In particular, the parallel ALS algorithms presented in [6, 7] and the parallel CCD++ algorithm presented in [9, 10] have in common that they distribute the *variables* and let each processor independently update its own subset of the variables. However, this comes at the cost of duplicating the storage for the incomplete matrix and, in the case of CCD++, also duplicating a significant portion of the work. Generalizing the approach to order N tensors would require N times the storage (and N times the work in the case of CCD++). In contrast, our algorithms are based on the idea of distributing the *incomplete tensor* instead of the variables and let the processors *collaboratively* update the variables. This approach does not suffer from the described problem and requires only a single copy of the incomplete tensor. Another benefit is an increase in the *degree of concurrency* (and hence improved scalability) from $\max_n\{I_n\}$ to the typically much larger $|\Omega|$.

The primary objects are the data tensor $\boldsymbol{\mathcal{A}}$, the CP tensor $\boldsymbol{\mathcal{X}}$, and in the case of CCD++ also the intermediate tensor $\boldsymbol{\mathcal{R}}$. In our parallel algorithms, the data tensor $\boldsymbol{\mathcal{A}}$ can have any arbitrary distribution. Let $\Omega = \Omega^{(1)} \cup \cdots \cup \Omega^{(p)}$ denote a partition of the index set Ω over p processors. Specifically, processor q owns $a_{\mathbf{i}}$ (and also $r_{\mathbf{i}}$ in the case of CCD++) for all $\mathbf{i} \in \Omega^{(q)}$. The factor matrices $\mathbf{X}^{(n)}$ for $n = 1, \ldots, N$ of the CP tensor $\boldsymbol{\mathcal{X}}$ are in both cases replicated on all p processors.

3.1. Parallel formulation of ALS

The inner loop of ALS (Algorithm 1) for mode n consists of constructing and solving I_n normal equations (5) of size $L \times L$. Each solve generates an updated row of the factor matrix $\mathbf{X}^{(n)}$ and the inner loop as a whole updates all rows of the matrix.

In our parallel formulation described in Algorithm 3, the processors construct local contributions to each of the I_n normal equations in parallel. These contributions are then summed up in a global reduction step to obtain the normal equations (5). Each processor

solves roughly $1/p$ of the normal equations and the updated rows of $\mathbf{X}^{(n)}$ are replicated in a global all-gather step.

Algorithm 3: Parallel formulation of ALS.

1 Initialize all vectors $\mathbf{x}_\ell^{(n)}$ in parallel;
2 **for** *each outer iteration* **do**
3 **for** $\hat{n} = 1, 2, \ldots, N$ **do**
4 Construct local contributions to each of the $I_{\hat{n}}$ normal equations (5) in the form of a local coefficient matrix $\mathbf{C}_{\hat{\imath}}$ of size $L \times L$ and a local right-hand side vector $\mathbf{d}_{\hat{\imath}}$ of length L for each $\hat{\imath} = 1, 2, \ldots, I_{\hat{\imath}}$;
5 Reduce (sum) and scatter the $I_{\hat{n}}$ normal equations defined by the pairs $(\mathbf{C}_{\hat{\imath}}, \mathbf{d}_{\hat{\imath}})$;
6 Solve the (roughly $I_{\hat{n}}/p$) local normal equations $(\mathbf{C}_{\hat{\imath}} + \lambda\mathbf{I})\mathbf{z}_{\hat{\imath}} = \mathbf{d}_{\hat{\imath}}$ for $\mathbf{z}_{\hat{\imath}}$;
7 Replicate the updated factor matrix $\mathbf{X}^{(\hat{n})}$;

In line 3 of Algorithm 3, the processors construct their local contributions in parallel. In line 4, the local contributions are reduced and the resulting normal equations are scattered over the processors. The normal equations are solved in parallel (but each one sequentially) in line 5, and the updated factor matrix is replicated in line 6.

Line 3 involves $\Theta(|\Omega|L^2)$ arithmetic operations and the degree of concurrency is $|\Omega|$. Line 5 involves $\Theta(I_{\hat{n}}L^3)$ arithmetic operations and the degree of concurrency is only $I_{\hat{n}}$. The load imbalance caused by line 5 near the limit of concurrency becomes more pronounced for higher ranks since the cost of line 5 grows like L^3 while the cost of line 3 grows only like L^2.

3.2. Parallel formulation of CCD++

The inner loop of CCD++ (Algorithm 2) consists of applying the update rule (6) to each of the $I_{\hat{n}}$ entries of the $\hat{\ell}$-th column $\mathbf{x}_{\hat{\ell}}^{(\hat{n})}$ of $\mathbf{X}^{(\hat{n})}$. Using the intermediate tensor $\boldsymbol{\mathcal{R}}$ defined in (7), the update rule can be expressed as

$$\left[\mathbf{x}_{\hat{\ell}}^{(\hat{n})}\right]_{\hat{\imath}} \leftarrow \frac{\alpha_{\hat{\imath}}}{\lambda + \beta_{\hat{\imath}}}, \quad \text{where} \quad \alpha_{\hat{\imath}} = \sum_{\substack{\mathbf{i}\in\Omega \\ i_{\hat{n}}=\hat{\imath}}} r_{\mathbf{i}}\gamma_{\hat{\imath}}, \quad \beta_{\hat{\imath}} = \sum_{\substack{\mathbf{i}\in\Omega \\ i_{\hat{n}}=\hat{\imath}}} \gamma_{\hat{\imath}}^2, \quad \gamma_{\hat{\imath}} = \prod_{\substack{n=1 \\ n\neq\hat{n}}}^{N} \left[\mathbf{x}_{\hat{\ell}}^{(n)}\right]_{i_n}. \tag{11}$$

Since the tensor $\boldsymbol{\mathcal{R}}$ has an arbitrary distribution, the data necessary to compute the tensor contractions in (11) for a fixed $\hat{\imath}$ are in general distributed over all processors. In our parallel formulation, the processors construct local contributions to the $2I_{\hat{n}}$ tensor contractions $\alpha_{\hat{\imath}}$ and $\beta_{\hat{\imath}}$ for $\hat{\imath} = 1, 2, \ldots, I_{\hat{n}}$. These contributions are then summed up in a global reduction step. Each processor updates roughly $I_{\hat{n}}/p$ of the entries of the vector $\mathbf{x}_{\hat{\ell}}^{(\hat{n})}$, and the updated vector is replicated in a global all-gather step. In other words, the parallel formulation of CCD++ is essentially analogous to the one for ALS. In addition, however, CCD++ also needs to initialize and update the intermediate tensor $\boldsymbol{\mathcal{R}}$. Since every factor matrix is replicated, the initialization, using (7), can be performed in a perfectly parallel manner without communication. The update, using (8), is also perfectly parallel for the same reason.

Algorithm 4: Parallel formulation of CCD++.

1 Initialize in parallel all vectors $\mathbf{x}_\ell^{(n)}$ and the intermediate tensor $\mathcal{R}$ for $\hat{\ell} = 1$ using (7);
2 **for** *each outer iteration* **do**
3 **for** $\hat{\ell} = 1, 2, \ldots, L$ **do**
4 **for** *each inner iteration* **do**
5 **for** $\hat{n} = 1, 2, \ldots, N$ **do**
6 Construct local contributions to each of the $2I_{\hat{n}}$ tensor contractions $\alpha_{\hat{\imath}}$ and $\beta_{\hat{\imath}}$ for $\hat{\imath} = 1, 2, \ldots, I_{\hat{n}}$;
7 Reduce (sum) and scatter the partial tensor contractions from the previous step;
8 Update the roughly $I_{\hat{n}}/p$ local entries of $\mathbf{x}_{\hat{\ell}}^{(\hat{n})}$;
9 Replicate the updated factor matrix column $\mathbf{x}_{\hat{\ell}}^{(\hat{n})}$;
10 Update $\mathcal{R}$ in parallel using (8) with $\hat{\ell}_{\text{old}} = \hat{\ell}$ and $\hat{\ell}_{\text{new}} = 1 + (\hat{\ell} \bmod L)$;

Algorithm 4 presents our parallel formulation of CCD++ in more detail. In line 1, the intermediate tensor $\mathcal{R}$ is initialized. In line 5, the processors construct in parallel their local contributions to the tensor contractions, and in line 6 the local contributions are summed up to obtain the tensor contractions necessary for the update rule (11). In line 7, the processors update the current column in parallel, and the updated column is replicated in line 8 in a global all-gather step. Finally, the tensor $\mathcal{R}$ is updated in line 9.

Line 5 involves $\Theta(|\Omega|)$ arithmetic operations and the degree of concurrency is $|\Omega|$. Line 7 involves $\Theta(I_{\hat{n}})$ arithmetic operations and the degree of concurrency is only $I_{\hat{n}}$. In contrast to ALS, the degree of concurrency is effectively limited by $|\Omega|$ in practice regardless of the rank.

4. Numerical Experiments

The parallel algorithms were tested on a distributed memory system. Each node is equipped with 48 cores distributed over four sockets. The nodes have a NUMA architecture consisting of eight NUMA locality domains per node with the six cores in each domain partially sharing a memory hierarchy.

In all experiments presented below, the factor matrices (3) were initialized with normally distributed random numbers and one inner iteration was used in CCD++. The tensor completion accuracy was measured on a randomly sampled test set of entries disjoint from the set Ω used in the training phase, and is measured by the root mean square error (RMSE) or the normalized root mean square error (NRMSE) (RMSE divided by the difference between maximum and minimum entry) on that set.

4.1. Synthetic data

We consider a random tensor $\mathcal{A} \in \mathbb{R}^{100\times100\times100\times100}$ with prescribed tensor rank $L \in \{10, 20, 30, 40, 50\}$, using exactly this rank in the algorithms. The aim was to investigate

the scalability of our parallel implementations of ALS and CCD++. The index set Ω was chosen randomly such that $|\Omega| = 10^6$ (1%) and λ was set to 10^{-3}. The number of cores were set to $p \in \{1, 6, 12, \ldots, 96\}$, that is, up to two full nodes were utilized. We stopped the CCD++ algorithm after 20 and ALS after 10 iterations, which leads to approximately the same execution time on a single core. The median execution time spent on one iteration was measured, including the evaluation of the objective function. Figures 1a and 1b show the resulting relative speedup as the number of cores increases. As expected (see Section 3.1), the scalability of ALS deteriorates with growing rank L, while CCD++ scales independently of L.

4.2. Applications

We now assess the performance of our parallel implementations of ALS and CCD++ for two data sets commonly used in the literature.

MovieLens 10M. The MovieLens 10M dataset[1] contains timestamped ratings of movies. Binning the time into 7-day wide bins results in a tensor of size $71\,567 \times 10\,677 \times 731$. The number of samples is $10\,000\,054$ (0.002%). Figures 2a and 2b report RMSE versus execution time on one core and one full node (48 cores), respectively, with rank $L = 40$ and $\lambda = 10^{-1}$. In this and the next example, the timings do not include the time needed for evaluating the test scores, which were instead obtained in separate runs using the same inputs. The two methods perform similarly on one core but CCD++ clearly outperforms ALS on 48 cores due to better parallel scaling.

Hyperspectral image. The hyperspectral image "Ribeira" [21] corresponds to a tensor of size $1017 \times 1340 \times 33$. The index set Ω was chosen randomly to contain 10% of the entries ($4\,497\,174$ samples). The test set is of the same cardinality. Figures 3a and 3b report NRMSE versus execution time on one core and one full node (48 cores), respectively, with $L = 100$ and $\lambda = 10^{-3}$. For this data, ALS is not only faster, but it also achieves a better reconstruction on the test set.

4.3. CCD++ with two inner iterations

We repeat the experiments from the previous section for the CCD++ algorithm with two instead of one inner iteration, in order to check if this results in any improvements. For both datasets, it turns out that the cost for two inner iterations is not compensated by the possibly improved rank-one approximations. The whole process slows down, as can bee seen in Figures 4a and 4b.

4.4. Function-related tensor

To account for the growing importance of function-related tensors in scientific computing [22], we have tested our algorithms on a tensor obtained from discretizing the function $\mathbf{x} \mapsto \exp(-\|\mathbf{x}\|_2)$, which has a cusp singularity at the origin, on a tensor product grid.

[1] `http://grouplens.org/datasets/movielens/`

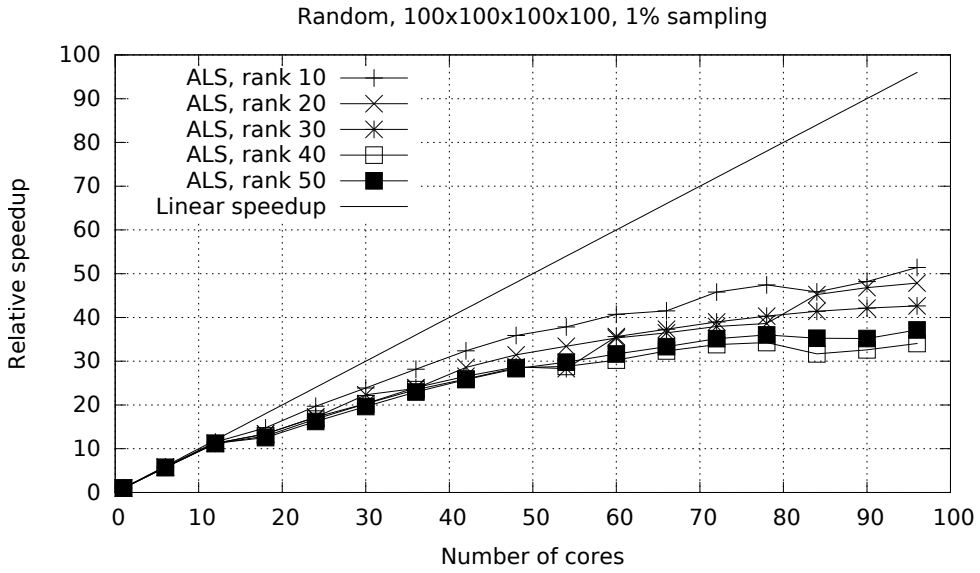

(a) Relative speed-up of ALS.

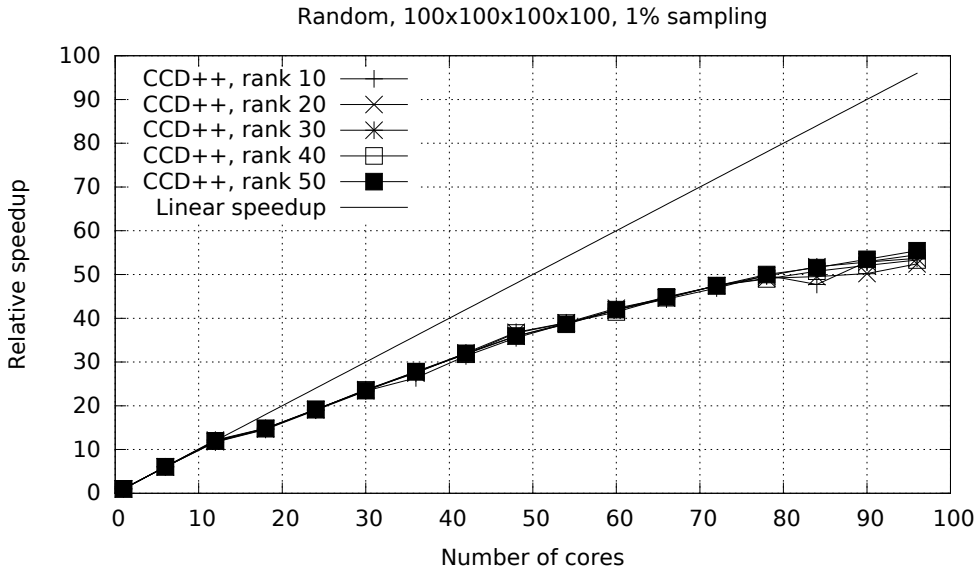

(b) Relative speed-up of CCD++.

Figure 1: Performance of parallel ALS and CCD++ for synthetic data.

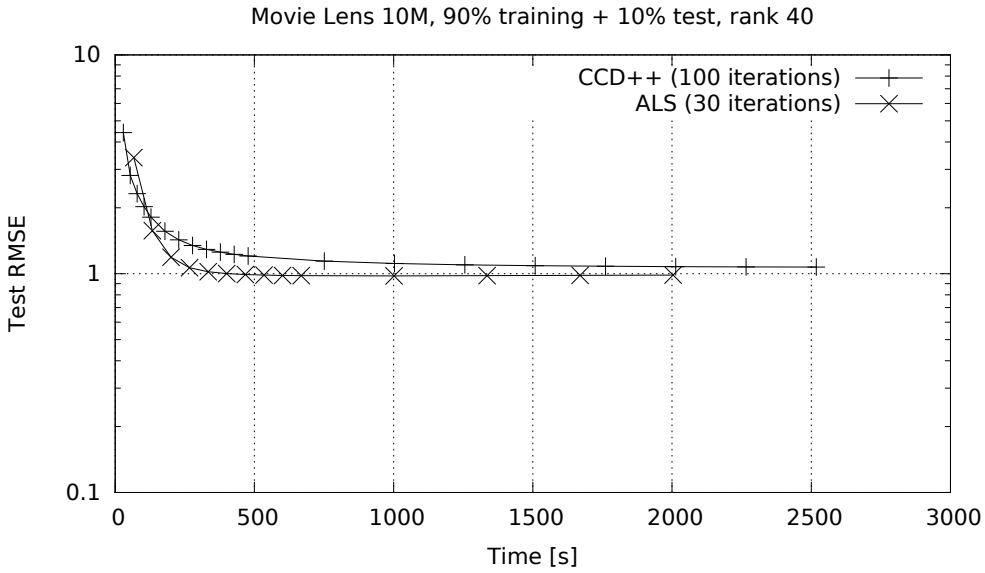

(a) Movie Lens 10M on 1 core.

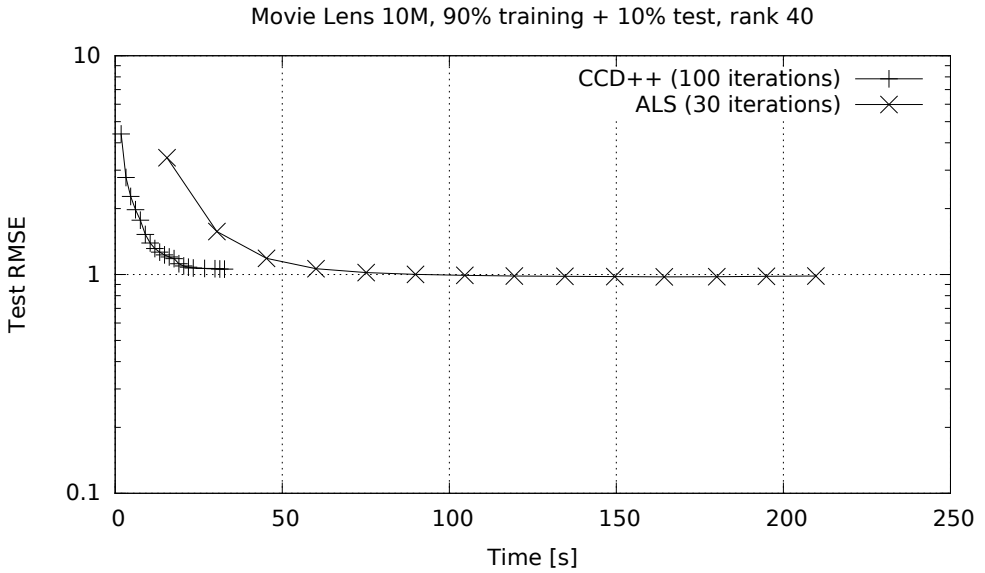

(b) Movie Lens 10M on 48 cores.

Figure 2: Performance of parallel ALS and CCD++ for the Movie Lens 10M data set.

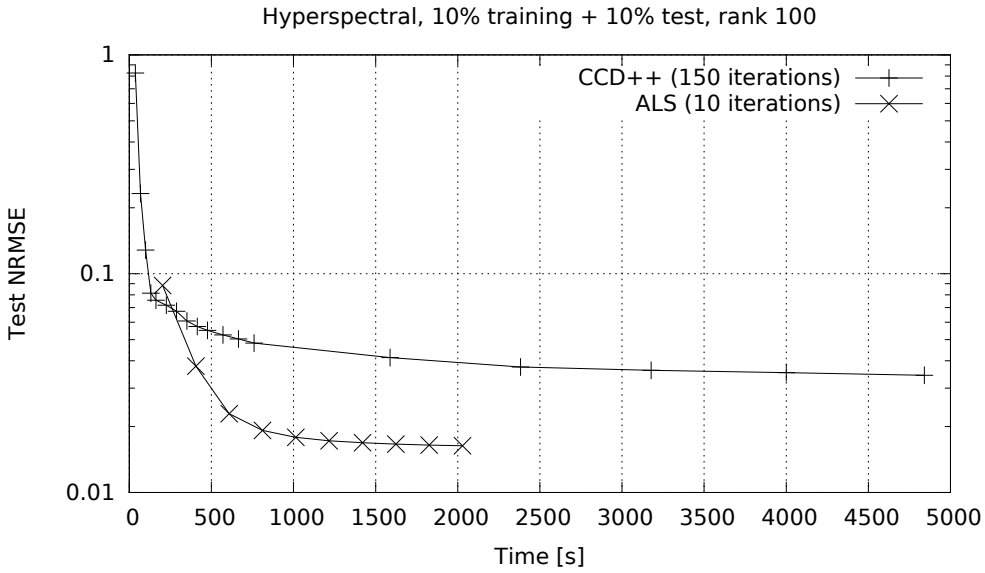

(a) Hyperspectral image on 1 core.

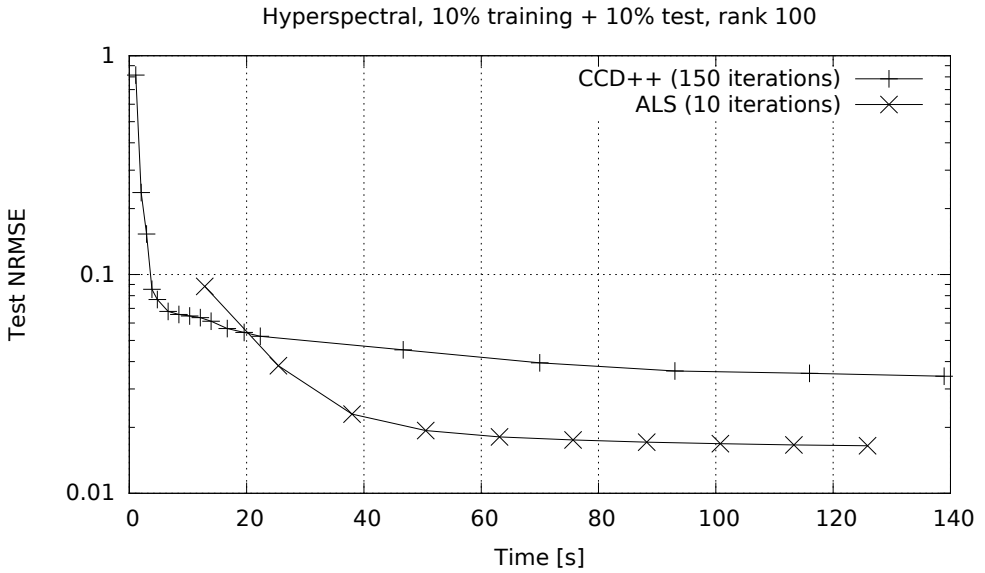

(b) Hyperspectral image on 48 cores.

Figure 3: Performance of parallel ALS and CCD++ for the hyperspectral image "Ribeira".

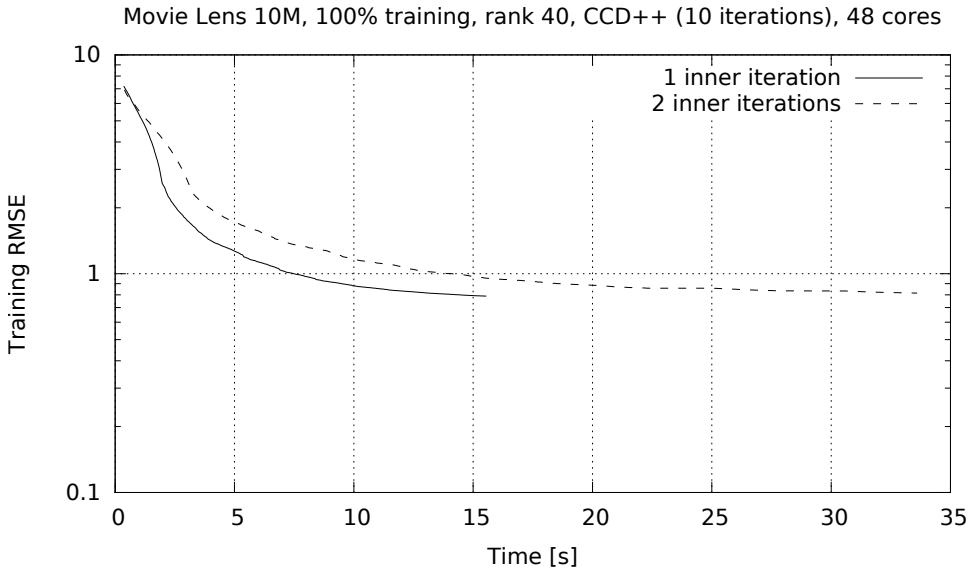

(a) Movie Lens 10M.

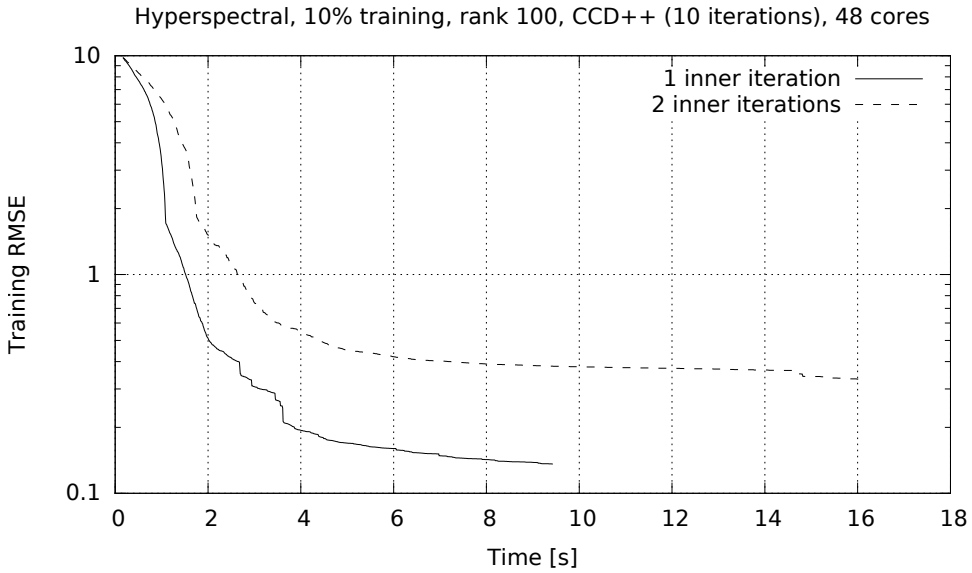

(b) Hyperspectral image.

Figure 4: One vs. two inner iterations of parallel CCD++.

Functions of this type play an important role as *Slater-type orbitals* in quantum chemistry. Tensor completion can be used, for example, to learn the entire function from a few function values.

The considered domain $[-1,1]^N$ is discretized by a regular grid with n^N grid points (an odd value n has been chosen such that the grid contains the origin). This gives a tensor $\boldsymbol{\mathcal{A}}$ with entries

$$a_{i_1,i_2,\ldots,i_N} = \exp(-\sqrt{\xi_{i_1}^2 + \xi_{i_2}^2 + \cdots + \xi_{i_N}^2})$$

where $\xi_{i_1}, \xi_{i_2}, \ldots, \xi_{i_N}$ are the grid points. We sample $10nNL$ entries of $\boldsymbol{\mathcal{A}}$ and apply our algorithms.

We used $N = 5$, $n = 51$, $L = 100$, and $10nNL = 255\,000$ samples in both methods. We have performed five trial runs with different random initial guesses. The resulting accuracies for the training phase are presented in Figures 5b and 5a. They suggest that ALS is more accurate and also less sensitive to the initial guess. For some trial runs CCD++ seems to offer a slight advantage in the initial phase.

5. Summary and conclusions

We have presented and analyzed two parallel algorithms (ALS and CCD++) for tensor completion in the CP format, provided convergence results for them, as well as numerical results on synthetic and real-world data. Concerning the comparison between the two algorithms, we have to draw a mixed conclusion. In contrast to CCD++, the parallel scalability of ALS appears to be sensitive to the prescribed CP rank and, consequently, CCD++ scales better than ALS for larger ranks when applied to random data. For data sets from specific applications, like hyperspectral images, we have observed on 48 cores that this disadvantage can be more than compensated by the faster convergence of ALS. For other applications, like MovieLens 10M, ALS is still slower. In terms of attained quality of approximation, ALS appears to be never worse and sometimes better than CCD++. In summary, this makes ALS one of the most powerful low-rank optimization algorithms currently at hand and CCD++ becomes a valuable alternative when scalability is critical.

Acknowledgments

Financial support has been provided by UMIT Research Lab via Balticgruppen and eSSENCE, a strategic collaborative eScience programme funded by the Swedish Research Council. This research was conducted using the resources of High Performance Computing Center North (HPC2N).

References

[1] T. G. Kolda, B. W. Bader, Tensor decompositions and applications, SIAM Rev. 51 (3) (2009) 455–500. doi:10.1137/07070111X.
URL http://dx.doi.org/10.1137/07070111X

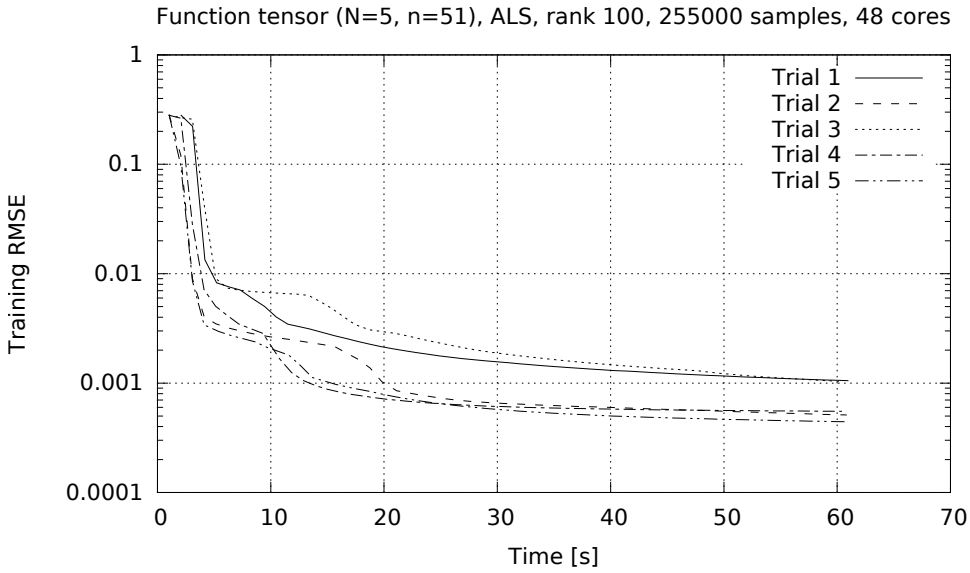

(a) ALS on the function tensor.

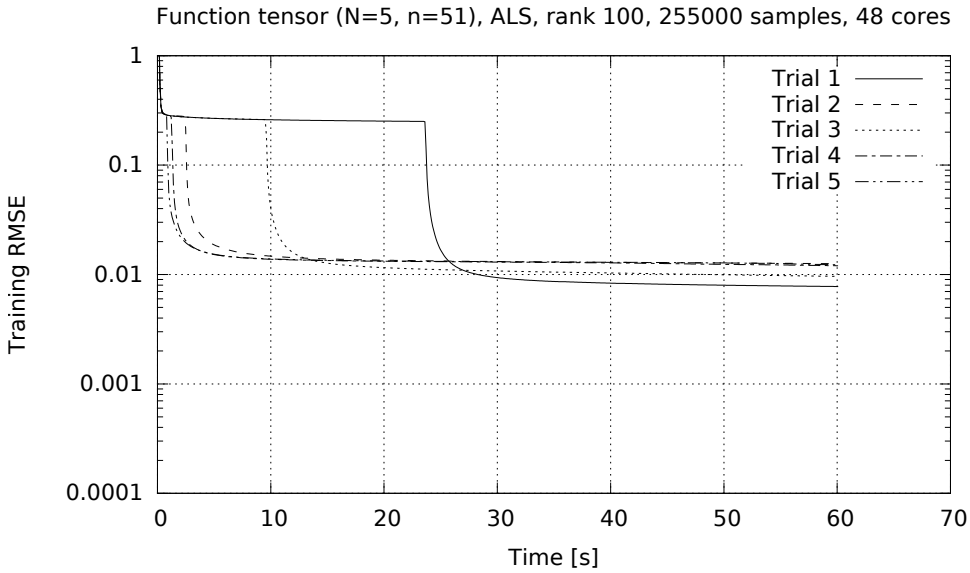

(b) CCD++.

Figure 5: Performance of parallel ALS and CCD++ for a function-related tensor.

[2] B. Hidasi, D. Tikk, Fast ALS-based tensor factorization for context-aware recommendation from implicit feedback, in: P. A. Flach, T. Bie, N. Cristianini (Eds.), Machine Learning and Knowledge Discovery in Databases, Springer, 2012, pp. 67–82. doi:10.1007/978-3-642-33486-3_5.
URL http://dx.doi.org/10.1007/978-3-642-33486-3_5

[3] G. Beylkin, J. Garcke, M. J. Mohlenkamp, Multivariate regression and machine learning with sums of separable functions, SIAM J. Sci. Comput. 31 (3) (2009) 1840–1857. doi:10.1137/070710524.
URL http://dx.doi.org/10.1137/070710524

[4] M. Signoretto, R. Van de Plas, B. De Moor, J. A. K. Suykens, Tensor versus matrix completion: A comparison with application to spectral data, IEEE Signal Proc. Let. 18 (7) (2011) 403–406.

[5] C. Da Silva, F. J. Herrmann, Hierarchical Tucker tensor optimization - applications to tensor completion, in: SampTA 2013, Bremen, Germany, 2013, pp. 384–387.

[6] C. Teflioudi, F. Makari, R. Gemulla, Distributed matrix completion, in: IEEE 12th International Conference on Data Mining, IEEE Computer Society, Los Alamitos, CA, USA, 2012, pp. 655–664. doi:http://doi.ieeecomputersociety.org/10.1109/ICDM.2012.120.

[7] Y. Zhou, D. Wilkinson, R. Schreiber, R. Pan, Large-scale parallel collaborative filtering for the Netflix prize, in: R. Fleischer, J. Xu (Eds.), Algorithmic Aspects in Information and Management, Springer, 2008, pp. 337–348. doi:10.1007/978-3-540-68880-8_32.
URL http://dx.doi.org/10.1007/978-3-540-68880-8_32

[8] I. Pilászy, D. Zibriczky, D. Tikk, Fast ALS-based matrix factorization for explicit and implicit feedback datasets, in: Proceedings of the Fourth ACM Conference on Recommender Systems, RecSys '10, ACM, New York, NY, USA, 2010, pp. 71–78. doi:10.1145/1864708.1864726.
URL http://doi.acm.org/10.1145/1864708.1864726

[9] H.-F. Yu, C.-J. Hsieh, S. Si, I. Dhillon, Scalable coordinate descent approaches to parallel matrix factorization for recommender systems, in: IEEE 12th International Conference on Data Mining, Los Alamitos, CA, USA, 2012, pp. 765–774. doi:http://doi.ieeecomputersociety.org/10.1109/ICDM.2012.168.

[10] H.-F. Yu, C.-J. Hsieh, S. Si, I. S. Dhillon, Parallel matrix factorization for recommender systems, Knowl. Inf. Syst.In press. doi:10.1007/s10115-013-0682-2.
URL http://dx.doi.org/10.1007/s10115-013-0682-2

[11] R. Gemulla, E. Nijkamp, P. J. Haas, Y. Sismanis, Large-scale matrix factorization with distributed stochastic gradient descent, in: Proceedings of the 17th ACM SIGKDD International Conference on Knowledge Discovery and Data Mining, ACM, 2011, pp. 69–77. doi:10.1145/2020408.2020426.
URL http://doi.acm.org/10.1145/2020408.2020426

[12] B. Recht, C. Ré, Parallel stochastic gradient algorithms for large-scale matrix completion, Math. Program. Comput. 5 (2) (2013) 201–226. doi:10.1007/s12532-013-0053-8.
URL http://dx.doi.org/10.1007/s12532-013-0053-8

[13] E. Acar, D. M. Dunlavy, T. G. Kolda, M. Morup, Scalable tensor factorizations for incomplete data, Chemometr. Intell. Lab. 106 (1) (2011) 41–56. doi:http://dx.doi.org/10.1016/j.chemolab.2010.08.004.
URL http://www.sciencedirect.com/science/article/pii/S0169743910001437

[14] G. Tomasi, R. Bro, PARAFAC and missing values, Chemometr. Intell. Lab. 75 (2) (2005) 163–180. doi:http://dx.doi.org/10.1016/j.chemolab.2004.07.003.
URL http://www.sciencedirect.com/science/article/pii/S0169743904001741

[15] Y. Xu, W. Yin, A block coordinate descent method for regularized multiconvex optimization with applications to nonnegative tensor factorization and completion, SIAM J. Imaging Sci. 6 (3) (2013) 1758–1789. doi:10.1137/120887795.
URL http://dx.doi.org/10.1137/120887795

[16] A. H. Phan, A. Cichocki, PARAFAC algorithms for large-scale problems, Neurocomputing 74 (11) (2011) 1970–1984. doi:http://dx.doi.org/10.1016/j.neucom.2010.06.030.
URL http://www.sciencedirect.com/science/article/pii/S0925231211000415

[17] V. de Silva, L.-H. Lim, Tensor rank and the ill-posedness of the best low-rank approximation problem,

SIAM J. Matrix Anal. Appl. 30 (3) (2008) 1084–1127. doi:10.1137/06066518X.
URL http://dx.doi.org/10.1137/06066518X

[18] A. Uschmajew, Local convergence of the alternating least squares algorithm for canonical tensor approximation, SIAM J. Matrix Anal. Appl. 33 (2) (2012) 639–652. doi:10.1137/110843587.
URL http://dx.doi.org/10.1137/110843587

[19] J. M. Ortega, W. C. Rheinboldt, Iterative solution of nonlinear equations in several variables, Academic Press, New York, 1970.

[20] Z. Q. Luo, P. Tseng, On the convergence of the coordinate descent method for convex differentiable minimization, J. Optim. Theory Appl. 72 (1) (1992) 7–35. doi:10.1007/BF00939948.
URL http://dx.doi.org/10.1007/BF00939948

[21] D. H. Foster, S. M. C. Nascimento, K. Amano, Information limits on neural identification of colored surfaces in natural scenes, Vis Neurosci. 21 (2004) 331–336, see http://personalpages.manchester.ac.uk/staff/david.foster/Hyperspectral_images_of_natural_scenes_04.html (Scene 7). doi:10.1017/S0952523804213335.
URL http://journals.cambridge.org/article_S0952523804213335

[22] L. Grasedyck, D. Kressner, C. Tobler, A literature survey of low-rank tensor approximation techniques, GAMM-Mitt. 36 (1) (2013) 53–78.

Recent publications:

MATHEMATICS INSTITUTE OF COMPUTATIONAL SCIENCE AND ENGINEERING
Section of Mathematics
Ecole Polytechnique Fédérale
CH-1015 Lausanne

24.2014 DANIEL KRESSNER, RAJESH KUMAR, FABIO NOBILE, CHRISTINE TOBLER:
Low-rank tensor approximation for high-order correlation functions of Gaussian random fields

25.2014 GIOVANNI MIGLIORATI, FABIO NOBILE:
Analysis of discrete least squares on multivariate polynomial spaces with evaluations in low-discrepancy point sets

26.2014 ABDUL-LATEEF HAJI-ALI, FABIO NOBILE, RAÚL TEMPONE:
Multi index Monte Carlo: when sparsity meets sampling

27.2014 ASSYR ABDULLE, ORANE JECKER:
An optimization-based multiscale coupling method

28.2014 LAURA IAPICHINO, ALFIO QUARTERONI, GIANLUIGI ROZZA, STEFAN VOLKWEIN:
Reduced basis method for the stokes equations in decomposable parametrized domains using greedy optimization

29.2014 ASSYR ABDULLE, PATRICK HENNING:
Localized orthogonal decomposition method for the wave equation with a continuum of scales

30.2014 DANIEL KRESSNER, ANDRÉ USCHMAJEW:
On low-rank approximability of solutions to high-dimensional operator equations and eigenvalue problems

31.2014 ASSYR ABDULLE, MARTIN HUBER:
Finite element heterogeneous multiscale method for nonlinear monotone parabolic homogenization problems

32.2014 ASSYR ABDULLE, MARTIN HUBER, GILLES VILMART:
Linearized numerical homogenization method for nonlinear monotone parabolic multiscale problems

33.2014 MARCO DISCACCIATI, PAOLA GERVASIO, ALFIO QUARTERONI:
Interface control domain decomposition (ICDD) methods for heterogeneous problems

34.2014 ANDRE USCHMAJEW:
A new convergence proof for the high-order power method and generalizations

35.2014 ASSYR ABDULLE, ONDREJ BUDÁC:
A Petrov-Galerkin reduced basis approximation of the Stokes equation in parametrized geometries

36.2014 ASSYR ABDULLE, MARTIN E. HUBER:
Error estimates for finite element approximations of nonlinear monotone elliptic problems with application to numerical homogenization

37.2014 LARS KARLSSON, DANIEL KRESSNER, ANDRÉ USCHMAJEW:
Parallel algorithms for tensor completion in the CP format